Amplification of intrinsic noise in a chaotic multimode laser system

C. Bracikowski, R. F. Fox, and Rajarshi Roy
School of Physics, Georgia Institute of Technology, Atlanta, Georgia 30332
(Received 29 July 1991)

The output intensity of an intracavity-frequency-doubled Nd: yttrium aluminum garnet (YAG) laser can exhibit chaotic variations under certain conditions. It has been predicted that the intrinsic noise due to spontaneous emission present in this laser system can be amplified by the chaotic dynamics. We report here the observation of noise amplification in a mathematical model of this laser system in a parameter regime that produces chaotic intensity variations. The amplification was observed in the evolution of the distribution of an ensemble of noisy trajectories, originating from identical initial conditions. The observed amplification occurred at a rate given by the largest Liapunov exponent and is consistent with the theoretical predictions of Fox and Keizer [Phys. Rev. A **43**, 1709 (1991)]. However, anomalous amplification was also observed and occurred at a rate ~ 10 times the Liapunov exponent. The mechanism for this effect is elucidated.

PACS number(s): 42.50.Lc

I. INTRODUCTION

When a nonlinear potassium titanyl phosphate (KTP) crystal is placed inside a Nd:YAG laser cavity, the output intensity can exhibit chaotic variations [1]. The nonlinear crystal converts some of the 1064-nm fundamental laser light into green light at ~ 532 nm by the processes of second-harmonic generation and sum-frequency generation. Sum-frequency generation creates nonlinear global coupling among the lasing modes (each mode is coupled to all other modes) which causes the laser output to vary periodically or chaotically under certain conditions. We have previously developed a deterministic rate equation model of this laser system which accurately reproduces the experimentally observed stable, periodic, and chaotic dynamics [2-5].

In this paper we present results which show the amplification of intrinsic noise in a parameter regime for which the laser equations produce chaotic intensity variations. A measure of this amplification is obtained by comparing the evolution of an ensemble of 20 noisy trajectories with a deterministic trajectory started from the same initial conditions. Fifteen sets of simulations were performed, each with a different noise strength. The noise strengths varied over 14 orders of magnitude. A plot of the mean time to reach a given separation between noisy trajectories and the deterministic one shows an exponential dependence on noise strength as was predicted by Fox and Keizer [6]. We find good agreement between the rate of the exponential separation and the calculated value of the Liapunov exponent for the dynamics.

In addition to the predicted noise amplification by the chaotic dynamics, we have observed an anomalous amplification of the noise that results in a trajectory separation rate about 10 times the Liapunov exponent.

In Sec. II the laser model that will be used in this paper is reviewed. The theory for the chaotic amplification of noise is discussed in Sec. III. We then describe the numerical observation of noise amplification in these rate equations in a parameter regime producing chaotic intensity variations. Section IV contains an analysis of these results, including a discussion of the mechanism responsible for the observed anomalous noise amplification.

II. LASER MODEL

We have previously developed a deterministic rate equation model of an intracavity-frequency-doubled Nd:YAG laser system which accurately reproduces the experimentally observed stable, periodic, and chaotic dynamics [2–5]. The model includes the polarizations of the cavity modes and the fact that the YAG rod may be birefringent. Figure 1 is a schematic of the intracavity doubled Nd:YAG laser we have modeled. The laser cavity contained a nonlinear KTP crystal which served as the frequency-doubling element. The intensity at the fundamental wavelength is highest within the laser cavity. Since the intensity of frequency-doubled light produced by the KTP crystal is proportional to the square of the intensity at the fundamental wavelength, the KTP crystal was placed inside the laser cavity. The laser is pumped by a ten-element phased-array laser diode with a maximum output power of 200 mW at around 810 nm. The highly divergent and elliptical pump beam is first collimated and then circularized before being focused into the cylindrical YAG rod by a 5-cm focal length lens. The

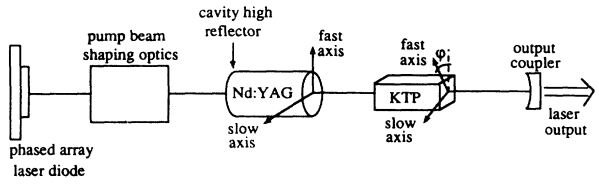

FIG. 1. Schematic of the diode-pumped Nd:YAG (neodymium doped yttrium aluminum garnet) laser with an intracavity KTP (potassium titanyl phosphate) crystal. The KTP crystal produces green light at half the wavelength of the fundamental emission (1064 nm) from the laser.

flat front face of the Nd:YAG crystal served as the cavity high reflector, and was coated to be highly reflecting at both the fundamental ($\sim$1064 nm, infrared) and doubled ($\sim$532 nm, green) wavelengths and highly transmitting at the pump wavelength. The KTP crystal was antireflection coated at both the fundamental and doubled wavelengths. The laser output coupler was highly transmitting at the doubled frequency and highly reflecting (>99.9%) at the fundamental, such that only the fundamental circulated in the laser cavity; the doubled frequency is simply transmitted by the output coupler. The Nd:YAG and KTP crystals were both 5 mm long and the entire laser cavity was about 3.5 cm long. The threshold pump power for this laser was about 10 mW.

As first pointed out by Oka and Kubota [7], a complete analysis of this laser system must include the polarizations of the cavity modes. These polarizations are given by the eigenvectors of the round-trip Jones matrix M for this laser cavity which are real and orthogonal [2]. These two eignevectors are the only two polarization states that are unchanged after one round trip in the cavity. Since the eigenvectors of the matrix M are real, the laser output will consist of linearly polarized components along one or both of the two orthogonal eigenvector directions.

Nd:YAG normally lases at 1064 nm in the infrared. However, the KTP crystal converts some of this fundamental light into green light at $\sim$532 nm. Green light is produced in the KTP crystal by second-harmonic generation from a single-cavity mode and by sum-frequency generation between pairs of modes. In second-harmonic generation, two photons from the same cavity mode of fundamental frequency ω combine to create one photon of green at frequency 2ω. In sum-frequency generation one photon from a cavity mode at frequency ω_1 and one photon from a different mode at frequency ω_2 combine to create one photon of green at frequency $(\omega_1+\omega_2)$. The amount of green light produced by sum-frequency generation depends on whether the contributing fundamental modes are polarized parallel or orthogonal to each other. The two processes for the generation of green light must be included in the laser rate equations as nonlinear loss terms for the fundamental intensity. The variations in the output intensity that are observed for some parameter values arise from the global coupling created among the lasing modes (each mode is coupled to every other mode) due to sum-frequency generation.

Each cavity mode can exist in one of the two orthogonal eigenpolarization directions, which we label as x and y. Let m and n be the number of modes polarized in the x and y directions, respectively, where $N=m+n$ is the total number of lasing modes. The deterministic rate equations for the fundamental intensities I_k and gains G_k are [2,8]

$$\tau_c\frac{dI_k}{dt}=\left[G_k-\alpha_k-g\epsilon I_k-2\epsilon\sum_{j(\neq k)}\mu_{jk}I_j\right]I_k\ ,$$
$$\tau_f\frac{dG_k}{dt}=\gamma-\left[1+I_k+\beta\sum_{j(\neq k)}I_j\right]G_k\ , \tag{1}$$

where τ_c (0.2 ns) and τ_f (240 μs) are the cavity round-trip time and fluorescence lifetime of the Nd^{3+} ion (the active ion in Nd:YAG), respectively; I_k and G_k are, respectively, the intensity and gain associated with the kth longitudinal mode; α_k is the cavity loss parameter for the kth mode; γ(0.05) is the small signal gain which is related to the pump rate above threshold; β (0.6) is the cross saturation parameter; and g (0.1) is a geometrical factor whose value depends on the angle between the YAG and KTP fast axes, as well as on the phase delays due to their birefringence. For modes having the same polarization as the kth mode, $\mu_{jk}=g$, while $\mu_{jk}=(1-g)$ for modes having the orthogonal polarization. This difference is due to the different amounts of sum-frequency generated green light produced by pairs of parallel polarized modes or by pairs of orthogonally polarized modes. Here, ϵ (5×10^{-6}) is a nonlinear coefficient whose value depends on the crystal properties of the KTP and describes the conversion efficiency of the fundamental intensity into doubled intensity. In these rate equations we have made the simplifying approximation that the gain γ (0.05) and cross saturation parameter β (0.6) are the same for all modes. The individual mode losses are assumed to differ only slightly, with $\alpha_k\sim0.01$. The parameter values given above represent typical experimental operating conditions.

As was mentioned earlier, these deterministic rate equations (1) have been found to accurately reproduce experimentally observed periodic and chaotic intensity variations. For the investigation of noise effects it is more convenient to use the entirely equivalent equations for the electric fields

$$\tau_c\frac{d(E_r)_k}{dt}=\left[G_k-\alpha_k-g\epsilon I_k-2\epsilon\sum_{j(\neq k)}\mu_jI_j\right]\frac{(E_r)_k}{2}\ ,$$
$$\tau_c\frac{d(E_i)_k}{dt}=\left[G_k-\alpha_k-g\epsilon I_k-2\epsilon\sum_{j(\neq k)}\mu_jI_j\right]\frac{(E_i)_k}{2}\ , \tag{2}$$
$$\tau_f\frac{dG_k}{dt}=\gamma-\left[1+I_k+\beta\sum_{j(\neq k)}I_j\right]G_k\ .$$

In the remainder of this paper we will discuss how intrinsic noise added into the rate equations is amplified when the model is integrated with parameter values which deterministically produce chaotic variations. This amplification is not present in the case of nonchaotic time traces.

III. AMPLIFICATION OF INTRINSIC NOISE BY CHAOTIC DYNAMICS

Reference [6] contains a detailed account of the theory for amplification of intrinsic noise by chaotic dynamics and of the technique employed to obtain accurate numerical simulations of this effect. To obtain the equations used in the numerical simulations, three steps are followed. In the first step, a mesoscopic master equation is constructed for the time evolution of a probability distribution, the mean values of which correspond to the macroscopic variables, i.e., the quantities I_k and G_k in the

present case. This probability distribution also describes the intrinsic fluctuations, or noise, associated with the macroscopic variables. Kurtz [6] has proved a limit theorem that yields a nonlinear Fokker-Planck equation that is a very accurate approximation to the full master equation. This Fokker-Planck equation constitutes the second step, and its diffusion terms determine the magnitudes of the intrinsic noise correlations. Numerically, both the master equation and the nonlinear Fokker-Planck equation are extremely difficult to implement efficiently. The third step recognizes that there exists a set of Langevin equations, equivalent to the nonlinear Fokker-Planck equation, in which the noise terms are predetermined by the correlations implied by the diffusion terms in the nonlinear Fokker-Planck equation (the fluctuation-dissipation relation in this context). When these correlations are independent of the state variables, i.e., the I_k, E_k, and G_k, the resulting Langevin equations have the form of the original macrovariable equations, Eqs. (2) in this case, with additive Gaussian white-noise terms, Eqs. (3) given below. The correlations of the noise sources are explicitly determined in the manner described above. Since the noise correlations can be determined without actually constructing the master equation, the first two steps may be bypassed, and one simply writes Eqs. (3) directly, as we do below. This is a consequence of the fact that the intrinsic noise is a result of spontaneous emission for which the correlations, Eqs. (4), are already known from earlier work.

Spontaneous emission noise in the laser is included as additive Gaussian white noise in the manner and for the reasons given above:

$$\tau_c \frac{d(E_r)_k}{dt} = \left[G_k - \alpha_k - g\epsilon I_k - 2\epsilon \sum_{j(\neq k)} \mu_j I_j \right] \left[\frac{(E_r)_k}{2} \right] + (f_1)_k ,$$

$$\tau_c \frac{d(E_i)_k}{dt} = \left[G_k - \alpha_k - g\epsilon I_k - 2\epsilon \sum_{j(\neq k)} \mu_j I_j \right] \left[\frac{(E_i)_k}{2} \right] + (f_2)_k , \quad (3)$$

$$\tau_f \frac{dG_k}{dt} = \gamma - \left[1 + I_k + \beta \sum_{j(\neq k)} I_j \right] G_k ,$$

where $(E_r)_k$ and $(E_i)_k$ are the real and imaginary parts of the electric field of the kth mode. Here $(f_1)_k$ and $(f_2)_k$ represent spontaneous emission noise and are Gaussian white (δ correlated) noise terms with the following properties:

$$\langle [f_i(t)]_k \rangle = 0 ,$$
$$\langle [f_i(t)]_k [f_j(s)]_m \rangle = 2D\delta_{ij}\delta_{km}\delta(t-s) , \quad (4)$$

where $i = 1,2$. The strength, $2D$, of the correlations is predetermined by the laser system.

In the integration of these field rate equations, the Gaussian distributed noise terms $(f_1)_k$ and $(f_2)_k$ are calculated using the Box-Muller method [9] from two uniform random deviates $(x_1)_k$ and $(x_2)_k$ on (0,1). When the discrete time step Δt used in the numerical integration is included, the noise terms $(f_1)_k$ and $(f_2)_k$ are given by

$$(f_1)_k = \sqrt{-4D\Delta t \ln[(x_1)_k]} \cos[2\pi(x_2)_k] ,$$
$$(f_2)_k = \sqrt{-4D\Delta t \ln[(x_1)_k]} \sin[2\pi(x_2)_k] \quad (5)$$

such that $(f_1)_k$ and $(f_2)_k$ have zero mean and variance equal to $2D$. The fact that the sine and cosine are used in Eqs. (5) means that $(f_1)_k$ and $(f_2)_k$ are uncorrelated. The fact that, for each k and at each time step two different uniform random deviates $(x_1)_k$ and $(x_2)_k$ are used, means that $(f_1)_k$ and $(f_i)_m$ are uncorrelated. This justifies Eqs. (4).

The integration of the stochastic equations (3) was carried out as follows. The deterministic equations (2) were numerically integrated using the IMSL subroutine DGEAR for intervals of 10 nsec. Noise terms were generated using the algorithm in Eqs. (5) with $\Delta t = 10$ nsec and added to the fields at the end of each interval. The parameter values used in the rate equations are given above in Sec. II. The field rate equations were integrated for various noise strengths from $2D = 10^{-20}$ to 10^{-6} sec^{-1}, each started with the same set of initial conditions. For each noise strength, 20 trajectories were calculated, each trajectory using a different set of random numbers to generate the noise. An integration without noise was also performed. For each noise strength, the total inten-

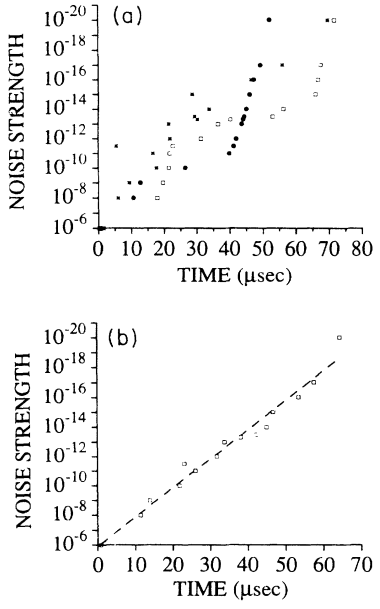

FIG. 2. (a) Time for the separation between noisy and deterministic trajectories produced by an integration of the numerical model to reach 1% of their mean saturated value. The three different symbols represent the different cases of initial conditions (discussed in the text) used in the calculations. (b) Mean time for the separation between noisy and deterministic trajectories produced by an integration of the numerical model to reach 1% of their mean saturated value. The rate of exponential separation is $\sim 4.6 \times 10^5$ sec^{-1}.

sity averaged over 20 realizations was compared with the total intensity for the deterministic trajectory to compute a separation parameter $S(t)$:

$$S(t)=\left|\left[\frac{1}{M}\sum_{k=1}^{M} I_k(t)\right]-I_0(t)\right|, \tag{6}$$

where M is the number of trajectories ($M=20$ in this case here), $I_k(t)$ is the intensity of the kth realization for a particular noise strength at time t, and $I_0(t)$ is the intensity of the deterministic trajectory at time t.

The time for the separation $S(t)$ to reach 1% of the mean saturated value was recorded. This calculation was repeated using the same noise strengths, but starting from a different set of initial conditions. A third set of calculations was done in which the initial conditions for each value of noise strength were different. This last integration was done in order to sample a wider domain of phase space. The mean separation time for each of these three calculations was determined. The time for the mean separation of the trajectories to reach 1% of the mean saturated value (the reference level) is plotted against noise strength in Fig. 2(a) for the three calculations just described. Figure 2(b) shows all three sets of data averaged together. It is very clear that the mean time to reach the reference level increases exponentially as the noise strength decreases, as predicted by Fox and Keizer, and the rate of this exponential increase is $\sim 4.6\times 10^5$ sec^{-1}. If the traditional linearized fluctuation theory were used instead, an average over an ensemble of sufficient size would yield zero for this difference. This is because the linearized theory predicts a symmetric Gaussian distribution of the stochastic trajectories about the deterministic trajectory. Kurtz's nonlinear fluctuation theory [6], however, predicts an asymmetric distribution not centered on the deterministic trajectory. In this case the average of the stochastic trajectories diverges exponentially from the chaotic deterministic trajectory at a rate given by the largest positive Liapunov exponent.

For two of these three cases of initial conditions, the average, largest Liapunov exponent was also computed for the noise strengths $2D=10^{-9}$, 10^{-13}, and 10^{-17} sec^{-1}. The largest Liapunov exponent for these three noise strengths in all the cases considered was about 3.3×10^4 sec^{-1}. The technique used here to compute the largest Liapunov exponent is discussed in Ref. [10]. However, the exponential rate of mean trajectory separation is about ten times larger than the largest Liapunov exponent. This discrepancy is explained below.

For the noise strengths of $2D=10^{-20}$ and 10^{-17} sec^{-1}, the average time for the separation to reach a variable reference level is found to increase exponentially as the reference level increases, as predicted by Fox and Keizer. The rate of this exponential increase is $\sim 2.8\times 10^5$ sec^{-1} and $\sim 2.3\times 10^5$ sec^{-1} for these two cases, respectively [Figs. 3(a) and 3(b)]. These rates are again about ten times the value of the largest Liapunov exponent.

This discrepancy can be understood by analyzing a plot

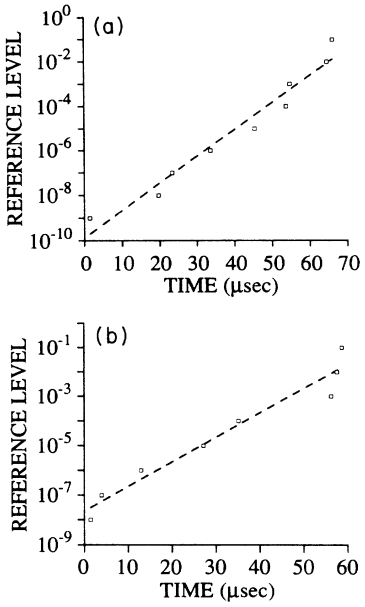

FIG. 3. (a) Mean time for the separation between noisy and deterministic trajectories produced from an integration of the numerical model to reach a variable reference level for a noise strength of $2D=10^{-20}$ sec^{-1}. The rate of exponential separation is $\sim 2.8\times 10^5$ sec^{-1}. (b) Mean time for the separation between noisy and deterministic trajectories produced from an integration of the numerical model to reach a variable reference level for a noise strength of $2D=10^{-17}$ sec^{-1}. The rate of exponential separation is $\sim 2.3\times 10^5$ sec^{-1}.

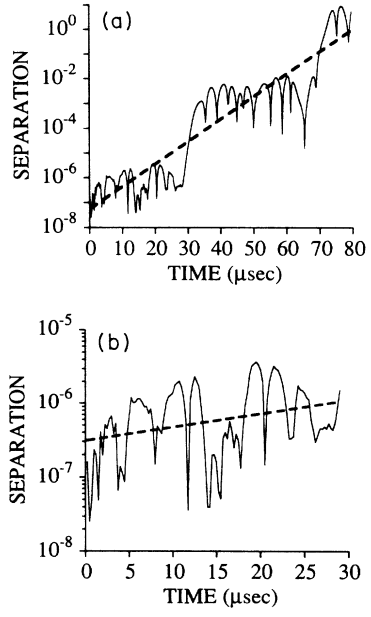

FIG. 4. (a) Separation of a noisy ($2D=10^{-17}$ sec^{-1}) and a deterministic trajectory with time. The rate of exponential separation is $\sim 2.1\times 10^5$ sec^{-1} which is the slope of the linear fit to the data (dashed line). This slope is approximately ten times the value of the largest Liapunov exponent calculated for the data. (b) Close-up view of Fig. 4(a). The rate of exponential separation is $\sim 4.2\times 10^4$ sec^{-1}, which is the slope of the linear fit to the data (dashed line). This slope is approximately equal to the value of the largest Liapunov exponent calculated for the data.

of the separation of a single noisy and the corresponding deterministic trajectory with time as shown in Fig. 4. Figure 4(a) shows that this separation saturates after about 80 μsec. The overall separation is observed to increase approximately exponentially at the rate of $\sim 2.1\times 10^{5}$ sec^{-1}, which is about the same as the rates of exponential increase discussed above. Note, however, the presence of sudden discrete steps in the difference between the two trajectories. The two steps in Fig. 4(a) occur at about 30 and 65 μsec. Furthermore, Fig. 4(b) shows that, in the first 30 μsec, just prior to the first step the separation increases approximately exponentially at the rate of $\sim 4.2\times 10^{4}$ sec^{-1}, which is about the same as the value of the largest Liapunov exponent calculated for the dynamics. The calculated value of the largest Liapunov exponent is only negligibly influenced by the presence of the steps since the time over which the steps occur is small relative to the time over which the calculation is performed. However, the time for the difference to reach the reference level is shortened due to the presence of the steps. If the steps did not occur then the separation of the deterministic and noisy trajectories would take place at a rate given by the largest Liapunov exponent just as in the case of the separation of two deterministic trajectories started from slightly different initial conditions (Fig. 5). The reason for the occurrence of the steps in the difference between noisy and deterministic trajectories is explained in Sec. IV.

The Liapunov exponent is the rate at which two initially close trajectories diverge in the complete phase space that is determined by all of the fields and gains. The separation between the total intensities of two deterministic trajectories whose initial intensities differ by 10^{-10} is plotted in Fig. 5. The fit to this data reveals an exponential separation at the rate of $\sim 3.23\times 10^{4}$ sec^{-1}, which is virtually the same as the Liapunov exponent calculated for the dynamics. Notice that no steps are observed in the plot of the separation. For comparison, when the laser equations are integrated with parameter values that yield a stable time trace, no exponential separation is observed between a noisy ($2D=10^{-10}$ sec^{-1}) and a deterministic trajectory as shown in Fig. 6. The difference plotted in Fig. 6 simply fluctuates about its saturation value of $\sim 5\times 10^{-3}$. When parameters yielding a chaotic trajectory were used, the saturation value of the separation was approximately unity [Fig. 4(a)].

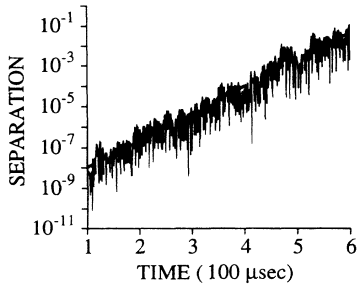

FIG. 5. Separation of two deterministic trajectories produced from an integration of the numerical model whose initial intensities differ by 10^{-10}. The rate of exponential separation is $\sim 3.2\times 10^{4}$ sec^{-1}. This rate is approximately equal to the value of the largest Liapunov exponent calculated for the data.

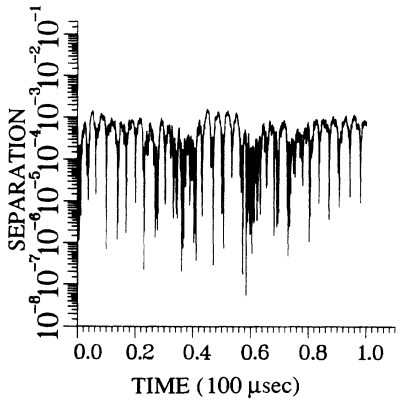

FIG. 6. Separation of a noisy ($2D=10^{-10}$ sec^{-1}) and a deterministic trajectory using parameter values that yield a stable time trace.

Even though gain variations are the driving force behind the intensity variations, the gain terms contribute negligibly to the value of the Liapunov exponent. The gain variations are only about 2% and the intensity variations are about 100% each relative to its respective mean value (Fig. 7). This explains why the exponential divergence rate in Fig. 5 is approximately equal to the Liapunov exponent even though only the total intensities are being considered. We have computed the value of the Liapunov exponent using all intensity and gain terms and using only the intensity terms and have found that they are identical up to eight decimal places.

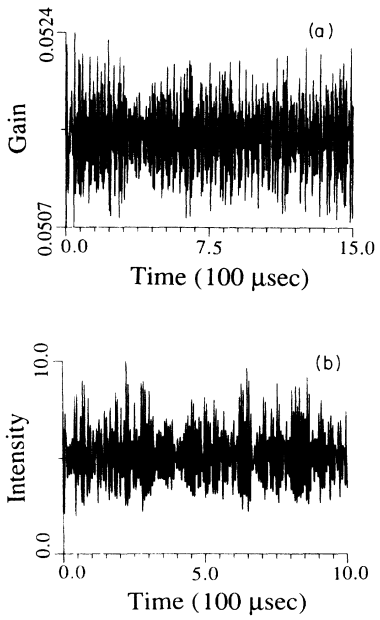

FIG. 7. (a) Gain variations produced from an integration of the numerical model. (b) Intensity variations produced from an integration of the numerical model.

IV. DISCUSSION

The discrepancy of a factor of 10 in the rate of amplification of noise in all of the data described above can be explained by the presence of the steps as shown in Fig. 4(a). It is a property of the laser dynamics here that some of the laser modes may occasionally turn off (perhaps due to the particular initial conditions) when the mode gain G_k remains less than the mode loss α_k for sufficiently long. Typically the modes with the higher losses, being closer to their threshold, will turn off more frequently then than lower loss modes. In a typical deterministic trajectory calculated here, if a mode turns off, the value of the intensity is reduced to an unphysically small value that is less than the spontaneous emission level in the laser. However, in the stochastic trajectory, the added noise prevents the intensity from decreasing to unphysical values such that, when $G_k-\alpha_k$ for that mode becomes positive, the mode will turn back on sooner and the exponential rate of this turn on is given by the value of $G_k-\alpha_k$. We have observed $G_k-\alpha_k$ to be fairly constant over the time in which the mode turns back on. In fact, the value of $G_k-\alpha_k$ is approximately ten times the Liapunov exponent.

We have observed that the large step at ~ 65 μsec [Fig. 4(a)] is caused by only one particular mode that turns off. It then turns back on in the stochastic trajectory (due to the additive noise) before it turns back on in the deterministic trajectory. The difference between the intensity value of this mode in the stochastic and deterministic trajectories was so large that it dominated the total difference between the trajectories, i.e., the total difference was slaved to the difference in this one mode.

It is thus possible to account for the anomalous amplification associated with the "steps." The remaining divergence of the initially close deterministic trajectories and the divergence of a stochastic trajectory (or an average over an ensemble of stochastic trajectories) from its deterministic relative both at a rate given by the Liapunov exponent are manifestations of the chaotic dynamics as predicted by Fox and Keizer [6].

In order to test the Fox and Keizer theory experimentally on a laser system, the laser noise strength must somehow be manipulated and some measurable quantity must be found whose value can change in the presence of noise when the laser is in a chaotic state. An experimental technique to control the amount of intrinsic noise in a laser has been described by Mussche and Siegman [11]. The nonorthogonality of the transverse modes in unstable resonator lasers and gain-guided lasers creates an enhancement of the linewidth and hence excess intrinsic noise. Mussche and Siegman have shown that the amount of excess noise can be changed by varying the geometrical magnification of an unstable resonator. This technique seems promising as an experimental method for examining the effect of spontaneous emission noise in a chaotic system.

In conclusion, the amplification of noise by the chaotic dynamics in the rate equation model of a multimode laser system has been observed. The separation of noisy and deterministic trajectories occurs at a rate given by the Liapunov exponent. In addition to this type of chaos-induced amplification, an anomalous amplification producing trajectory separations at about ten times the value of the Liapunov exponent has also been observed. This effect is a result of the fact that a mode turns on faster with added noise than without, and is not related to the presence of chaos.

ACKNOWLEDGMENTS

We acknowledge support from NSF Grant No. ECS 8722216 (C.B. and R.R.), NSF Grant No. PHY-9043227 (R.F.F.), and AFOSR Grant No. 90-0158 (R.F.F.).

[1] T. Baer, J. Opt. Soc. Am. B **3**, 1175 (1986).
[2] G. E. James, E. M. Harrell, II, C. Bracikowski, K. Wiesenfeld, and R. Roy, Opt. Lett. **15**, 1141 (1990).
[3] K. Wiesenfeld, C. Bracikowski, G. E. James, and R. Roy, Phys. Rev. Lett. **65**, 1749 (1990).
[4] C. Bracikowski and R. Roy, Phys. Rev. A **43**, 6455 (1991).
[5] C. Bracikowski and R. Roy, Chaos **1**, 49 (1991).
[6] R. F. Fox and J. Keizer, Phys. Rev. A **43**, 1709 (1991).
[7] M. Oka and S. Kubota, Opt. Lett. **13**, 805 (1988).
[8] G. E. James, Ph.D. dissertation, Georgia Institute of Technology, 1990 (unpublished).
[9] W. H. Press, B. P. Flannery, S. A. Teukolsky, and W. T. Vetterling, *Numerical Recipes: The Art of Scientific Computing* (Cambridge University, Cambridge, 1989), p. 202.
[10] A. J. Lichtenberg and M. A. Lieberman, *Regular and Stochastic Motion* (Springer-Verlag, Berlin, 1983), p. 264.
[11] (a) A. E. Siegman, Phys. Rev. A **39**, 1253 (1989); (b) **39**, 1264 (1989); (c) P. L. Mussche and A. E. Siegman, Proc. SPIE **1376**, 153 (1990).